Materials Research Proceedings **26** (2023) 109-114 https://doi.org/10.21741/9781644902431-18

Fractional viscoelastic characterization of laminated glass

Luca Viviani[1, a *], Mario Di Paola[2, b] and Gianni Royer-Carfagni[1, c]

[1]Departement of Engineering and Architecture, University of Parma, Parma, Italy

[2]Departement of Engineering, University of Palermo, Palermo, Italy

[a]luca.viviani@unipr.it, [b]mario.dipaola@unipa.it, [c]gianni.royer@unipr.it

Keywords: Laminated Glass, Fractional Viscoelastic Modelling, Blast Loading

Abstract. Glass façades are often required to withstand against explosive events due to premeditated or accidental causes. Laminates made by glass plies bonded by thin polymeric foils (laminated glass) need to be used to avoid catastrophic breakage. The paradigmatic case study considered is that of a rectangular three-layer laminate, made of two glass plies, modelled as Kirchhoff-Love plates, sandwiching a thin viscoelastic polymeric interlayer. Its time-dependent response under the action of a blast wave is described via fractional calculus operators, whose main advantage is that only two material constants are needed for an exhaustive characterization. The dynamic equations are treated à la Galërkin and their integration in time relies on the Grünwald-Letnikov approach. The fractional characterization presents noteworthy advantages from a computational point of view. We find that the maximum stress peak is mildly affected by the viscosity of the interlayer, which instead dictates the subsequent rebounding oscillations.

Viscoelastic properties of polymeric interlayer

Laminated glass is a composite formed by two (or more) glass plies sandwiching one (or more) polymeric foil(s), permanently bonded with a process at high temperature and pressure in autoclave. The polymeric interlayer is too thin to present bending capacity, but it contributes to the stiffness and strength of the laminate by coupling the glass plies [1, 2]. Its viscoelastic behavior is characterized by the relaxation function $R(t)$. Since the lamination process in autoclave can modify the mechanical properties of the interlayer, the relaxation curve should be measured directly on laminated glass samples. Shear relaxation tests are usually performed but, for practical reasons, the observation period shall be in an interval varying from a minimum of a few seconds to a maximum of a few weeks. Further details about the experimental procedures can be in found in [3] and [4]. The extrapolation to smaller/larger time scales can be done on the basis of Time–Temperature Superposition (TTS) principle, according to which a variation of the testing temperature is associated with a variation of the time scale for the viscosity effects [5]. For most commercial polymers, the typical shape of $R(t)$, in the bi-logarithmic stress–time plane, is as indicated in Figure 1: it presents two pseudo-linear branches, connected by a transition zone. Figure 1 Qualitative plot of a typical relaxation function $R(t)$. The first branch is fitted by a power law (straight line), which allows to analytically extrapolate the values at time scales of the same order of the characteristic load duration TdUnder the impulsive action of a blast wave, the branch of interest is certainly that on the left hand side of the graph. As represented in the figure, this branch can be analytically fitted by a power law (linear trend in the bi-log scale) of the form

$$R(t) = \frac{C_\alpha}{\Gamma(1-\alpha)} t^{-\alpha}, \tag{1}$$

where $\Gamma(\cdot)$ is the Euler's Gamma function, C_α[MPa s$^\alpha$] is a dimensional coefficient, and α the number associated with the slope of the line in the bi-log graph.

Materials Research Proceedings **26** (2023) 109-114 https://doi.org/10.21741/9781644902431-18

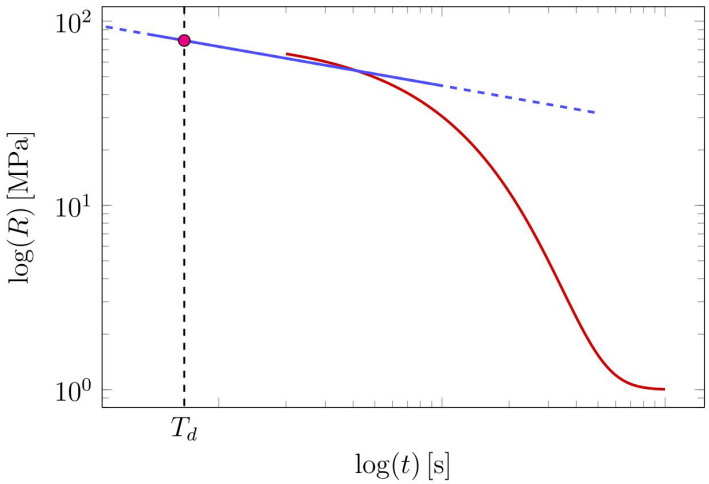

Figure 1 Qualitative plot of a typical relaxation function R(t). The first branch is fitted by a power law (straight line), which allows to analytically extrapolate the values at time scales of the same order of the characteristic load duration T_d of the blast wave.

The structural model for laminated plates

The schematic representation of the composite plate is shown in Figure 2. This is a three-layer plate composed by two thick elastic plies (layers ‘‘1’’ and ‘‘2’’) sandwiching one thin viscoelastic core (layer ‘‘0’’). A reference frame is introduced: the (x, y) axes are located in-plane, while the z axis indicates the out-of-plane direction, with the mid-surface of each layer corresponding to $z = 0$. The external plies are subjected only to the bending contribution; while the core produces the shear coupling under the assumption that there is no sliding at the interfaces. The thickness of the external plies is denoted by h_i with $i = 1, 2$, so that the distance between the mid-planes reads $\bar{h} = h_0 + (h_1 + h_2)/2$, where h_0 represents the thickness of polymeric core. With reference to Figures 2(b) and 2(c), the interlayer ‘‘0’’ undergoes shear strains, which depend on the in-plane displacements $u_i = u_i(x, y, t)$ and $v_i = v_i(x, y, t)$ of the external layers, for $i = 1, 2$, as well as the out-of-plane displacement $w = w(x, y, t)$, which is the same for both layers. For a constitutive model based on fractional calculus, the shear forces per unit length $Q_{x,0}$ and $Q_{y,0}$ depend on the shear stresses $\tau_{xz,0} = \tau_{xz,0}(x, y, t)$ and $\tau_{yz,0} = \tau_{yz,0}(x, y, t)$, in the form

$$Q_{x,0} = Q_{x,0}(x, y, t) = \int_{-h_0/2}^{h_0/2} \tau_{xz,0}\, dz = C_{\alpha_0}\, {}_0^C\mathcal{D}_t^\alpha \left[u_2 - u_1 + \bar{h}\frac{\partial w}{\partial x}\right](t), \tag{2.1}$$

$$Q_{y,0} = Q_{y,0}(x, y, t) = \int_{-h_0/2}^{h_0/2} \tau_{yz,0}\, dz = C_{\alpha_0}\, {}_0^C\mathcal{D}_t^\alpha \left[v_2 - v_1 + \bar{h}\frac{\partial w}{\partial y}\right](t), \tag{2.2}$$

where ${}_0^C\mathcal{D}_t^\alpha[\dots]$ denotes Caputo’s fractional derivative of order α, with $0 < \alpha < 1$, defined as

$$ {}_0^C\boldsymbol{\mathcal{D}}_t^{\boldsymbol{\alpha}}[\boldsymbol{f}(\cdot)](\boldsymbol{t}) = \frac{\mathbf{1}}{\boldsymbol{\Gamma(1-\alpha)}} \int_0^t (\boldsymbol{t} - \bar{\boldsymbol{t}})^{-\boldsymbol{\alpha}}\, \dot{\boldsymbol{f}}(\bar{\boldsymbol{t}})\, \boldsymbol{d\bar{t}}.$$

Materials Research Proceedings **26** (2023) 109-114 https://doi.org/10.21741/9781644902431-18

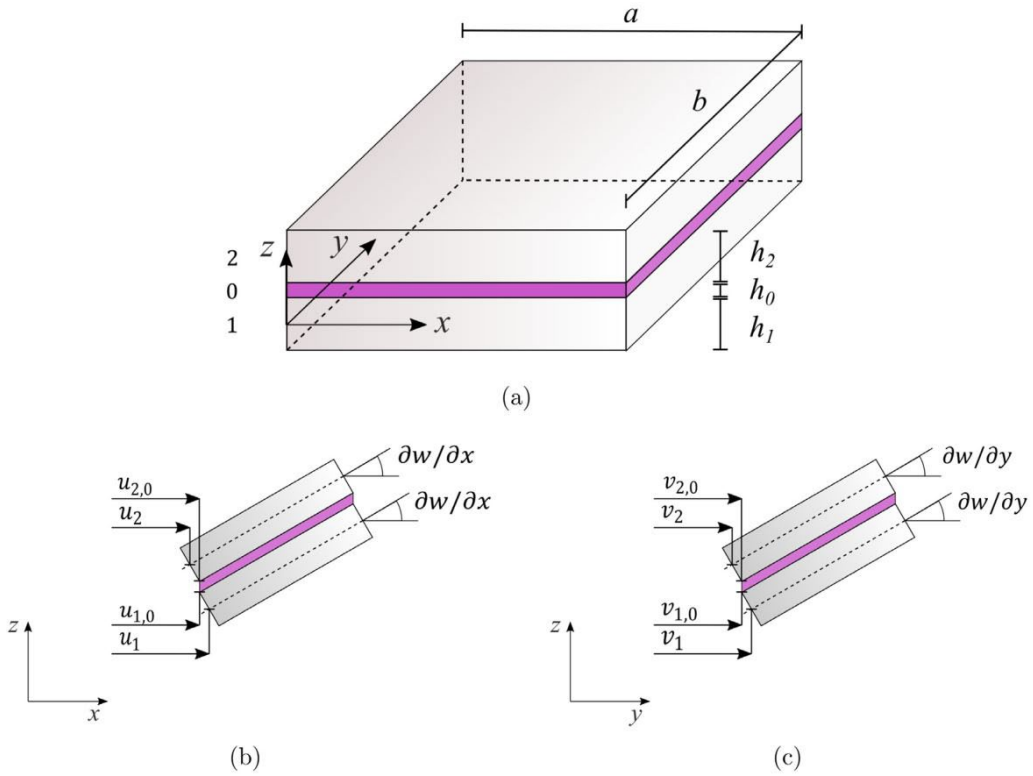

Figure 2 Schematic representation of a three-layer laminated glass plate. The glass plies are denoted as ''1'' and ''2'', while the core is the layer ''0''. For each layer, the reference system is located at one corner of the corresponding middle plane, with the z axis in the out-of-plane direction. The figure shows (a) the undistorted reference configuration and (b) the $\boldsymbol{x} - \boldsymbol{z}$ *view and the (c)* $\boldsymbol{y} - \boldsymbol{z}$ *view of the deformed configuration of the plate, with indication of the variables used to describe the displacement field.*

The glass plates are modelled according to Kirchhoff-Love plate theory, with Young's modulus $E_1 = E_2 \equiv E_g$ and Poisson's ratio $\nu_1 = \nu_2 \equiv \nu$, and with the same thickness ($h_2 = h_1 \equiv h$). Their dimensions are indicated as $a \times b \times h$. The inertia of the laminate is accounted by means of the global mass per unit area μ. Due to the geometric and load symmetry, $u_1 = -u_2$ and $v_1 = -v_2$. Hence, setting $\Delta u = u_2 - u_1$ and $\Delta v = v_2 - v_1$, the problem is described by the three dynamic equations [6]

$$\begin{aligned}\mu\frac{\partial^2 w(x,y,t)}{\partial t^2} + \frac{E_g h^3}{6(1-\nu^2)}\left(\frac{\partial^4 w(x,y,t)}{\partial x^4} + 2\frac{\partial^4 w(x,y,t)}{\partial x^2\,\partial y^2} + \frac{\partial^4 w(x,y,t)}{\partial y^4}\right) \\ = \frac{\bar{h}}{h_0} C_{\alpha_0}{}^{C}\mathcal{D}_t^{\alpha}\left[\frac{\partial \Delta u(x,y,\cdot)}{\partial x} + \bar{h}\frac{\partial^2 w(x,y,\cdot)}{\partial x^2}\right](t) \\ + \frac{\bar{h}}{h_0} C_{\alpha_0}{}^{C}\mathcal{D}_t^{\alpha}\left[\frac{\partial \Delta v(x,y,\cdot)}{\partial y} + \bar{h}\frac{\partial^2 w(x,y,\cdot)}{\partial y^2}\right](t) + p(t)\end{aligned} \tag{3.1}$$

$$\begin{aligned}\frac{E_g h}{1-\nu^2}\left[\frac{\partial^2 \Delta u(x,y,t)}{\partial x^2} + \frac{1}{2}(1-\nu)\frac{\partial^2 \Delta u(x,y,t)}{\partial y^2} + \frac{1}{2}(1+\nu)\frac{\partial^2 \Delta v(x,y,t)}{\partial x\,\partial y}\right] \\ = \frac{2}{h_0} C_{\alpha}{}_0{}^{C}\mathcal{D}_t^{\alpha}\left[\Delta u(x,y,\cdot) + \bar{h}\frac{\partial w(x,y,\cdot)}{\partial x}\right](t),\end{aligned} \tag{3.2}$$

Materials Research Proceedings **26** (2023) 109-114 https://doi.org/10.21741/9781644902431-18

$$\frac{E_g h}{1-\nu^2}\left[\frac{\partial^2 \Delta v(x,y,t)}{\partial y^2}+\frac{1}{2}(1-\nu)\frac{\partial^2 \Delta v(x,y,t)}{\partial x^2}+\frac{1}{2}(1+\nu)\frac{\partial^2 \Delta u(x,y,t)}{\partial x \partial y}\right] = \frac{2}{h_0} C_\alpha \, {}_0^C\mathcal{D}_t^\alpha \left[\Delta v(x,y,\cdot)+\bar{h}\frac{\partial w(x,y,\cdot)}{\partial y}\right](t), \tag{3.3}$$

where

$$p(t) = p_r\left(1-\frac{t}{T_d}\right)e^{-\beta\frac{t}{T_d}} \tag{4}$$

represents the loading action interpreted via Friedlander equation [7]. We set $p_r = 80$ kPa as peak overpressure, $T_d = 12.7 \cdot 10^{-3}$ s as time positive duration and $\beta = 0.95$ denotes the decay coefficient. The time history recalls that classified as EXV25, in accordance with the standard ISO 16933:2007 [8]. In order to solve the set of equilibrium equations for a simply supported plate, the unknown variables and the loading action are expressed in double Fourier sine series, in the form

$$w(x,y,t) = \sum_{m=1}^{M}\sum_{n=1}^{N} w_{mn}(t)\sin\left(\frac{m\pi x}{a}\right)\sin\left(\frac{n\pi y}{b}\right) \tag{5.1}$$

$$\Delta u(x,y,t) = \sum_{m=1}^{M}\sum_{n=1}^{N} \Delta u_{mn}(t)\cos\left(\frac{m\pi x}{a}\right)\sin\left(\frac{n\pi y}{b}\right) \tag{5.2}$$

$$\Delta v(x,y,t) = \sum_{m=1}^{M}\sum_{n=1}^{N} \Delta v_{mn}(t)\sin\left(\frac{m\pi x}{a}\right)\cos\left(\frac{n\pi y}{b}\right) \tag{5.3}$$

$$\Delta v(x,y,t) = \sum_{m=1}^{M}\sum_{n=1}^{N} \Delta v_{mn}(t)\sin\left(\frac{m\pi x}{a}\right)\cos\left(\frac{n\pi y}{b}\right) \tag{5.4}$$

This choice automatically fulfils the boundary conditions for a simply supported plate along the perimeter with in-plane free edges. By substituting them in the solving system (3.1)-(3.3), we can find the time dependent functions (modes $m-n$) $w_{mn}(t)$, $\Delta_{mn}(t)$ and $\Delta v_{mn}(t)$ with a step-by-step numerical integration, relying on the Grünwald-Letnikov approach [9] for fractional derivatives. The imposed initial conditions are $w_{mn}(t) = \Delta u_{mn}(t) = \Delta v_{mn}(t) = 0$ for $t < 0$.

Numerical experiments

The geometric and mechanical parameters for the considered laminated plate are $\boldsymbol{a \times b \times h_i = 1 \times 1 \times 0.01}$ m^3, $\boldsymbol{i = 1,2}$, $\boldsymbol{h_0 = 2.28}$ mm, $\boldsymbol{E_g = 70}$ GPa, $\boldsymbol{\nu = 0.25}$, densities $\boldsymbol{\rho = 2500}$ kg/m^3 and $\boldsymbol{\rho_0 = 1000}$ kg/m^3. The constitutive properties for three different types of interlayer, labelled as materials A B and C, according to the experimental campaign of [10] are: $\boldsymbol{\alpha = 0.155}$, $\boldsymbol{C_\alpha = 0.474}$ MPa s$^\alpha$ (material A); $\boldsymbol{\alpha = 0.117}$, $\boldsymbol{C_\alpha = 9.409}$ MPa s$^\alpha$ (material B); $\boldsymbol{\alpha = 0.117}$, $\boldsymbol{C_\alpha = 84.138}$ MPa s$^\alpha$ (material C). In order to understand how the hereditary memory of viscoelasticity contributes to the dynamic response, it is interesting to compare the bending stress $\boldsymbol{\sigma_{xx}}$ with the correspondent solution for perfectly elastic interlayers. The stress is evaluated at the plate center $\boldsymbol{(x,y) = (a/2, b/2)}$, on the external surface not directly invested by the pressure wave. The relaxation functions are assumed to be power laws and these are represented by inclined straight lines on bi-log plane; the equivalence with an elastic material (quasi-elastic approximation) is done by considering for it a shear modulus corresponding to the value of the relaxation curve at characteristic duration of the load $\boldsymbol{T_d}$. Graphically, the elastic

Materials Research Proceedings **26** (2023) 109-114 https://doi.org/10.21741/9781644902431-18

behavior corresponds to a horizontal line ($\alpha = 0$), which intersects the relaxation function at $\boldsymbol{t = T_d}$, where $\boldsymbol{T_d = 12.7 \cdot 10^{-3}}$ s is the time duration of the compression phase provided by Friedlander equation (4). Hence, the elastic limit corresponds to $\boldsymbol{R(t) = C_0}$ which, for the cases at hand, corresponds to $\boldsymbol{C_0 = 0.835}$ MPa for material A, $\boldsymbol{C_0 = 14.484}$ MPa for material B, $\boldsymbol{C_0 = 129.516}$ MPa for material C. The results to be compared are reported in Figure 3 for the three considered interlayers.

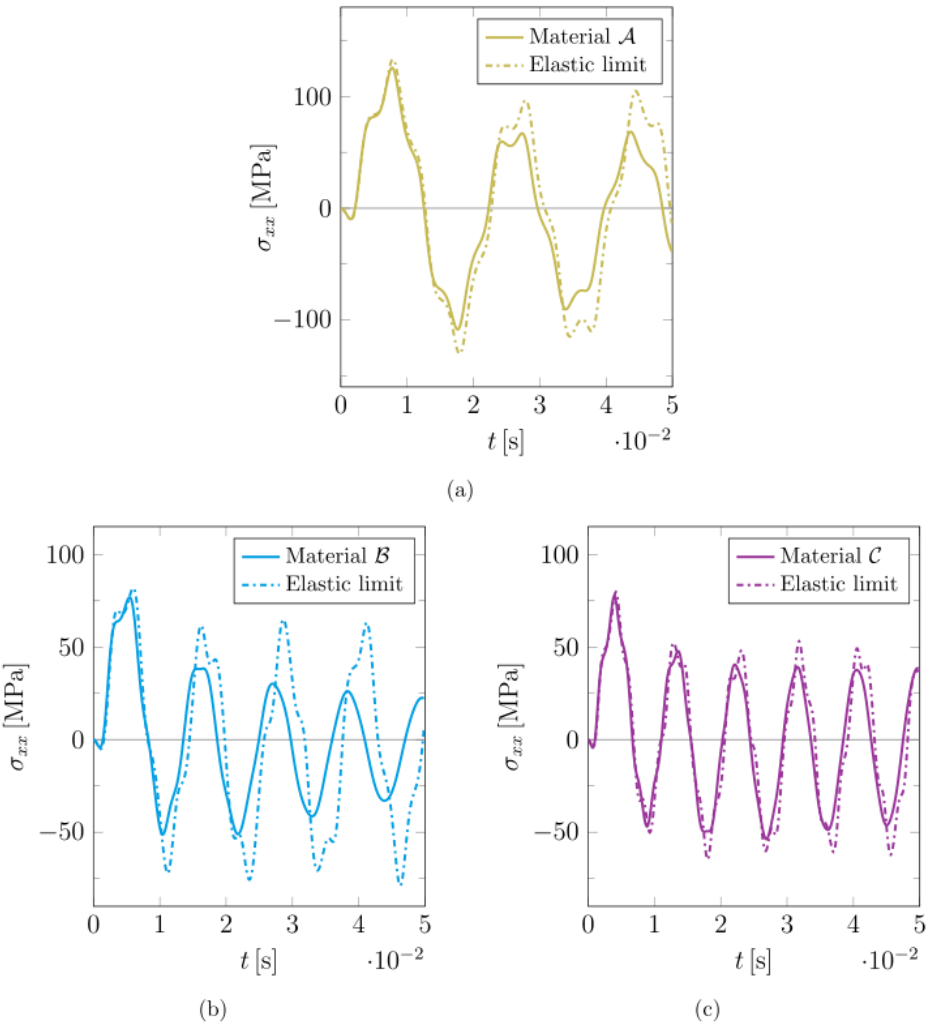

Figure 3 Stress component $\boldsymbol{\sigma_{xx}}$ evaluated at the centre of ply 2 at $\boldsymbol{z = -h/2}$. The plate is simply supported along its edges, and it is subjected to the blast pressure $\boldsymbol{p(t)}$. The corresponding solutions are compared with the quasi-elastic approximation. (a) Interlayer of type A; (b) interlayer B; (c) interlayer C.

In all the cases, there is a good superimposition between viscoelastic and elastic responses for what concerns the first peak. If we consider the response in a broader time interval, the difference is minimal when the interlayer is made of material C, the stiffest of all, inasmuch the monolithic limit (rigid shear coupling of the plies) is attained. Materials A and B provide a similar response: the dissipation due to the viscous component decreases the magnitude of the successive peaks and slightly increases the frequency of oscillations. With the interlayer is of type A, the sandwich is more compliant; hence, there are less oscillations within the considered time interval if compared with the other materials.

Conclusions

The case study is represented by a three-layer plate, where two elastic glass plies sandwich a thin polymeric foil without bending capacity, but sufficient to provide the shear coupling of the glass plies. The novelty of the presented analysis consists in the fractional constitutive model used for the interlayer. If compared with the more classic viscoelastic description via Prony series, the fractional approach is more straightforward and computationally advantageous, since only two parameters are needed to characterize the material response. The numerical experiments have accounted for three different polymeric interlayers, so to obtain a spectrum of dynamic responses in terms of stress. Under impulsive loading, the first (maximum) peak is not qualitatively affected by the viscosity of the interlayer, which however significantly lowers the values of the subsequent rebounding peaks. The greatest limitation of this model is represented by the assumption of linear elastic model à la Kirchhoff–Love for the glass plates, therefore neglecting the geometric non-linearities, which certainly play a role under high deformations. The extension to a non-linear model will represent the subject of future work.

References

[1] L. Galuppi G. Royer-Carfagni, "The post-breakage response of laminated heat-treated glass under in plane and out of plane loading," *Composites Part B: Engineering,* vol. 147, pp. 227-239, 2018. https://doi.org/10.1016/j.compositesb.2018.04.005

[2] I. V. Ivanov, "Analysis, modelling, and optimization of laminated glasses as plane beam," *International Journal of Solids and Structures,* vol. 43, pp. 6887-6907, 2'006. https://doi.org/10.1016/j.ijsolstr.2006.02.014

[3] M. López-Aenlle A. Noriega F. Pelayo, "Mechanical characterization of polyvinil butyral from static and modal tests on laminated glass beams," *Composites Part B: Engineering,* vol. 169, pp. 9-18, 2019. https://doi.org/10.1016/j.compositesb.2019.03.077

[4] X. Centelles F. Pelayo M. J. Lamela-Rey A. I. Fernandez R. Salgrado-Pizarro J. R. Castro L. F. Cabeza, "Viscoelastic characterization of seven laminated glass interlayer materials from static tests," *Construction and Building Materials,* vol. 279, p. 122503, 2021. https://doi.org/10.1016/j.conbuildmat.2021.122503

[5] M. L. Williams R. F. Landel J. D. Ferry, "The temperature dependence of relaxation mechanisms in amorphous polymers and other glass-forming liquids," *Journal of the American Chemical society,* vol. 77, pp. 3701-3707, 1955. https://doi.org/10.1021/ja01619a008

[6] L. Viviani M. Di Paola G. Royer-Carfagni, "A fractional viscoelastic model for laminated glass sandwich plates under blast actions," *International Journal of Mechanical Sciences,* vol. 222, p. 107204, 2022. https://doi.org/10.1016/j.ijmecsci.2022.107204

[7] P. S. Bulson, Explosive loading of engineering structures, CRC Press, 1997. https://doi.org/10.4324/9780203473863

[8] Iintenrational Organization of Standards (ISO 16933:2007), Glass in building—Explosion-resistant security glazing—Test and classification for arena air-blast loading, 2007.

[9] I. Podlubny, Fractional Differential Equations, Academic Press, 1998.

[10] L. Biolzi S. Cattaneo M. Orlando L. Ruggero Piscitelli P. Spinelli, "Constitutive relationships of different interlayer materials for laminated glass," *Composite Structures,* vol. 244, p. 112221, 2020. https://doi.org/10.1016/j.compstruct.2020.112221